JBC RESEARCH ARTICLE

Structural and functional insights into the inhibition of human voltage-gated sodium channels by μ-conotoxin KIIIA disulfide isomers

Received for publication, September 27, 2021, and in revised form, February 8, 2022 Published, Papers in Press, February 12, 2022,
https://doi.org/10.1016/j.jbc.2022.101728

Hue N. T. Tran[1], Kirsten L. McMahon[1], Jennifer R. Deuis[1], Irina Vetter[1,2,*], and Christina I. Schroeder[1,3,*]

From the [1]Institute for Molecular Bioscience, The University of Queensland, St Lucia, Queensland, Australia; [2]School of Pharmacy, The University of Queensland, Woolloongabba, Queensland, Australia; [3]Center for Cancer Research, National Cancer Institute, National Institutes of Health, Frederick, Maryland, USA

Edited by Mike Shipston

μ-Conotoxins are components of cone snail venom, well-known for their analgesic activity through potent inhibition of voltage-gated sodium channel (Na_V) subtypes, including $Na_V1.7$. These small, disulfide-rich peptides are typically stabilized by three disulfide bonds arranged in a 'native' CysI-CysIV, CysII-CysV, CysIII-CysVI pattern of disulfide connectivity. However, μ-conotoxin KIIIA, the smallest and most studied μ-conotoxin with inhibitory activity at $Na_V1.7$, forms two distinct disulfide bond isomers during thermodynamic oxidative folding, including Isomer 1 (CysI-CysV, CysII-CysIV, CysIII-CysVI) and Isomer 2 (CysI-CysVI, CysII-CysIV, CysIII-CysV), but not the native μ-conotoxin arrangement. To date, there has been no study on the structure and activity of KIIIA comprising the native μ-conotoxin disulfide bond arrangement. Here, we evaluated the synthesis, potency, sodium channel subtype selectivity, and 3D structure of the three isomers of KIIIA. Using a regioselective disulfide bond-forming strategy, we synthetically produced the three μ-conotoxin KIIIA isomers displaying distinct bioactivity and Na_V subtype selectivity across human Na_V channel subtypes 1.2, 1.4, and 1.7. We show that Isomer 1 inhibits Na_V subtypes with a rank order of potency of $Na_V1.4 > 1.2 > 1.7$ and Isomer 2 in the order of $Na_V1.4 \approx 1.2 > 1.7$, while the native isomer inhibited $Na_V1.4 > 1.7 \approx 1.2$. The three KIIIA isomers were further evaluated by NMR solution structure analysis and molecular docking with $hNa_V1.2$. Our study highlights the importance of investigating alternate disulfide isomers, as disulfide connectivity affects not only the overall structure of the peptides but also the potency and subtype selectivity of μ-conotoxins targeting therapeutically relevant Na_V subtypes.

Pain, in particular neuropathic and inflammatory, is of major medical concern worldwide. Voltage-gated sodium channels (Na_Vs) have been proven to play an essential role in many different pain states in animal and human models (1–7). There are nine sodium channel subtypes ($Na_V1.1$–$Na_V1.9$) currently described, all sharing a common overall structural motif (8). Most neurons express multiple sodium channel isoforms with $Na_V1.1$ (9), $Na_V1.2$ (10), $Na_V1.3$ (11, 12) and $Na_V1.6$ (13) being expressed in the central nervous system, while $Na_V1.4$ and $Na_V1.5$ are expressed in skeletal (14) and cardiac muscles (15), respectively. $Na_V1.7$ (16), $Na_V1.8$ (17), and $Na_V1.9$ (3) subtypes are preferentially expressed in the peripheral nervous system. These peripheral sodium channels have been genetically validated to be modulating neuronal excitability associated with different types of pain, including nociception (17, 18), neuropathic pain (3, 5, 18, 19) and acute inflammation (8, 16, 20, 21). Thus, peripheral Na_V subtypes, such as $Na_V1.7$, are potential targets for the development of novel analgesics.

Conotoxins from the venom of marine cone snails are considered prospective drug leads because of their potency, Na_V subtype selectivity, and analgesic efficacy in animal and human trials (1, 22). μ-Conotoxins are 14 to 26 amino acid residue peptides that share a specific cysteine framework of $CCX_nCX_nCX_nCC$ (23–25). The μ-conotoxin super family comprises five branches, termed M-1 to M-5, based on the number of residues in the third cystine loop between the fourth and fifth cysteine residues (25). With a framework including six cysteine residues, the μ-conotoxins can theoretically form 15 different disulfide bond isomers. However, μ-conotoxins isolated directly from cone snail venom are typically found to adopt a CysI-CysIV, CysII-CysV, CysIII-CysVI conformation, which has accordingly been accepted as the 'native' fold of the μ-conotoxin family (25). However, if isolated peptide material is not available for coelution with synthetic material, for example, when peptide sequences are identified from cDNA venom duct libraries, using proteomics or transcriptomics, or when the peptide is not present, or expressed at very low levels in the venom, it can be challenging to ascertain the native fold of the peptide. Accordingly, some recent reports have shown that it is not always the 'native' conotoxin peptide fold that is the more potent biologically active peptide, and conotoxins with non-native disulfide bond connectivity can outperform the presumed 'native' counterpart (26–28). For example, synthetic μ-PIIIA, a μ-conotoxin identified from the cDNA of the venom duct of the cone *Conus purpurascens* (26), formed three active isomers under

* For correspondence: Christina I. Schroeder, christina.schroeder@nih.gov; Irina Vetter, i.vetter@imb.uq.edu.au.

thermodynamic oxidative folding conditions with the non-native isomer of PIIIA (CysI-CysV, CysII-CysVI, CysIII-CysIV) being slightly more potent than the PIIIA isomer comprising the native μ-conotoxin disulfide-bond arrangement (27). A similar peculiarity has been observed within the α-conotoxin family, where a non-native disulfide bond isomer of the 15-residue α-conotoxin AuIB (comprising two disulfide bonds) was 10-fold more potent than the native fold of the peptide (28). Discoveries such as these emphasize the importance, but also the potential, of further investigation into the activity of different disulfide bond connectivities of these small, highly disulfide-rich peptides and how different disulfide connectivities of the same peptide can influence not only potency but also receptor subtype selectivity. Herein, we focus our investigation on three different disulfide-bond isomers of μ-KIIIA, one of the most extensively investigated μ-conotoxins targeting $Na_V1.7$ (29, 30).

KIIIA is a 16-residue μ-conotoxin, identified from a cDNA venom duct library of *Conus kinoshitai* that acts by blocking the pore of Na_Vs (20, 31–33). KIIIA is the smallest μ-conotoxin identified to date (34), comprising only one residue in loop 1 of the peptide, compared to 4 to 6 for other μ-conotoxins (Table 1). Like other μ-conotoxins in the family, KIIIA has been reported to most potently inhibit rat $Na_V1.2$ and rat $Na_V1.4$ (29, 30, 35). However, unlike most μ-conotoxins, KIIIA also inhibits the peripheral analgesic target $Na_V1.7$ with nanomolar affinity (29, 30). Upon initial synthetic production, KIIIA was reported to form one major isomer during thermodynamic folding (31), which was assumed to comprise the native μ-conotoxin disulfide connectivity (CysI-CysIV, CysII-CysV, CysIII-CysVI). A later study by Khoo *et al.* (35) reported two isomers during thermodynamic folding, and by carrying out direct mass spectrometric collision-induced dissociation fragmentation, it was identified that in fact neither of the two isomers observed during thermodynamic folding were KIIIA comprising the native μ-conotoxin fold (35). Instead, the two synthetically produced KIIIA isomers comprised CysI-CysV, CysII-CysIV, CysIII-CysVI connectivity (thermodynamic Isomer 1, referred to as Isomer 1-T) as the primary peak and CysI-CysVI, CysII-CysIV, CysIII-CysV connectivity (thermodynamic Isomer 2, referred to as Isomer 2-T) as the minor peak, with the minor isomer reported to be five times less potent than Isomer 1 against $rNa_V1.2$ (35). Indeed, as of yet, there has been no studies on KIIIA comprising the native μ-conotoxin disulfide connectivity of CysI-CysIV, CysII-CysV, CysIII-CysVI.

KIIIA and other small μ-conotoxins have been shown to exhibit analgesic properties in mouse inflammatory pain assays (20, 29, 36) and it is believed that the size and framework of μ-conotoxins, coupled with their high affinity and unique Na_V channels selectivity, make them prospective therapeutic agents suitable for the development of novel analgesic drugs (22, 25, 29, 37–44). To better understand the structure and activity of KIIIA isomers and the influence of different disulfide connectivity on Na_V affinity and subtype selectivity, we chemically produced three isomers of KIIIA including Native, Isomer 1, and Isomer 2 using a regioselective oxidation strategy. Our results revealed differences in Na_V subtype selectivity and potency between the three disulfide isomers that could partially, albeit not wholly, be explained by structural studies and molecular modeling.

Results

Synthesis

KIIIA and analogs were assembled using 9-fluorenylmethoxycarbonyl (Fmoc) solid phase peptide chemistry. Unprotected KIIIA was thermodynamically oxidized in 0.1 M NH_4HCO_3, pH 8, 100 eq GSH, and 10 eq GSSG producing two distinct isomers (Isomer 1-T and Isomer 2-T, where T stands for thermodynamic) (Fig. 1*A*) that showed similar relative retention times and peak height ratios as those observed by Khoo *et al.* (35) The two thermodynamically folded isomers, Isomer 1-T and Isomer 2-T, were readily isolated by reverse-phase HPLC (RP-HPLC). To ensure correct disulfide bond-formation, regioselective synthesis of each isomer producing the desired connectivity was carried out (Isomer 1-R and Isomer 2-R, where R stands for regioselective). However,

Table 1
Sequences of peptides belonging to the μ-conotoxin family

μ-conotoxins	Sequences	References
KIIIA	CC---N----CSSKWCRDHSRCC*	(31)
KIIIB	NGCC---N----CSSKWCRDHSRCC*	(31, 35)
SIIIA	ZNCC---NG--GCSSKWCRDHARCC	(31, 92, 93)
SIIIB	ZNCC---NG--GCSSKWCKDHARCC	(93)
SmIIIA	ZRCC---NGRRGCSSRWCRDHSRCC*	(76)
GIIIA	RDCC--TOOKK-CKDRQCKOO-RCCA*	(94)
GIIIB	RDCC--TOORK-CKDRRCKOM-KCCA*	(94)
GIIIC	RDCC--TOOKK-CKDRRCKOL-KCCA*	(94)
TIIIA	RHGCC--KGOKG-CSSRECROQH-CC*	(93)
PIIIA	RLCC--GFOKS-CRSRQCKOH-RCC*	(26, 27)
BuIIIA	VTDRCC-K-NGKRGCG-RWCRDHSRCC*	(95)
BuIIIB	VGERCC-K-NGKRGCG-RWCSSHSRCC*	(95)
BuIIIC	IVDRCCNKGNGKRGC-SRWCRDHSRCC	(95)
CIIIA	GRCC---EGPNGCSSRWCKDHARCC*	(96)
CnIIIA	GRCC---DVPNACSSKWCRDHARCC*	(96)
CnIIIB	ZGCC---GEPNLCFTRWCRNNARCCRQQ*	(96)
MIIIA	ZGCC---NVPNGCSGRWCRDHAQCC	(96)
SxIIIC	RGCC---NGRGGCSSRWCRDHARCC*	(53)

*, C-terminal amidation; Z, pyroglutamate; O, hydroxyproline; KIIIA highlighted in gray; Cys residues highlighted in yellow.

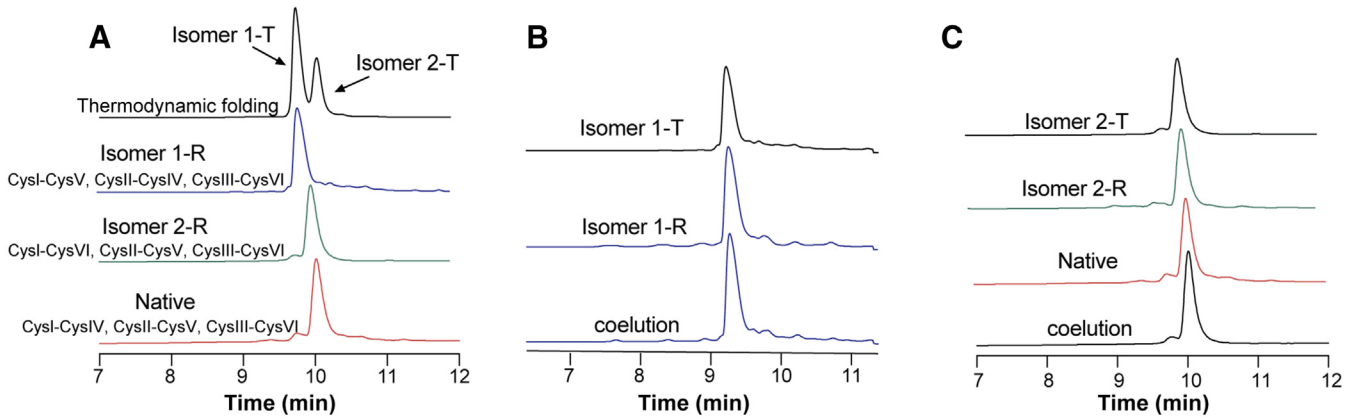

Figure 1. Analytical RP-HPLC traces showing disulfide bond isomers of KIIIA obtained through thermodynamic oxidation and isomers obtained through step-wise directed folding conditions. *A*, Isomer 1-T and Isomer 2-T formed in thermodynamic condition (*black*), directed Isomer 1-R (*blue*), Isomer 2-R (*green*), and Native (*red*) conformation. *B*, Isomer 1-T (*black*) coeluted with Isomer 1-R (CysI-CysV, CysII-CysIV, CysIII-CysVI) (*blue*). *C*, Isomer 2-T coeluted with both directed Isomer 2-R (CysI-CysVI, CysII-CysIV, CysIII-CysV) (*green*) and Native (CysI-CysIV, CysII-CysV, CysIII-CysVI) isomer (*red*) and was ultimately assigned as Isomer 2-R based on NMR. RP-HPLC, reverse-phase HPLC.

directing the disulfide connectivity of KIIIA proved challenging (Table S1 and Figs. S1–S3) and after trialing a variety of regioselective protecting group strategies including 4-methyltrityl/dimethylphosphinyl/S-acetamidomethyl (Acm), S-triphenylmethyl (Trt)/p-methoxybenzyl (Mob)/Acm, Trt/Acm/4-methylbenzyl (Mebzl), and Trt/Acm/Mob, we found that only the combination of using Cys with protecting groups Trt to form the first disulfide bond, Acm to form the second disulfide bond followed by 4,4′-dimethylsulfinylbenzhydryl (Msbh) to form the final third disulfide bond, successfully produced Native KIIIA (Table S1 and Fig. 2). Using this orthogonal cysteine-protecting group strategy, we were subsequently able to produce Isomer 1-R (CysI-CysV, CysII-CysIV, CysIII-CysVI), Isomer 2-R (CysI-CysVI, CysII-CysIV, CysIII-CysV), and Native (CysI-CysIV, CysII-CysV, CysIII-CysVI) KIIIA with ∼10% yield from crude peptides (Table S2 and Fig. S4).

Assignment of disulfide bond connectivity by coelution

Linear KIIIA formed two isomers during thermodynamic oxidation, as shown by analytical HPLC (Fig. 1*A*). The major peak, Isomer 1-T, coeluted with regioselectively synthesized

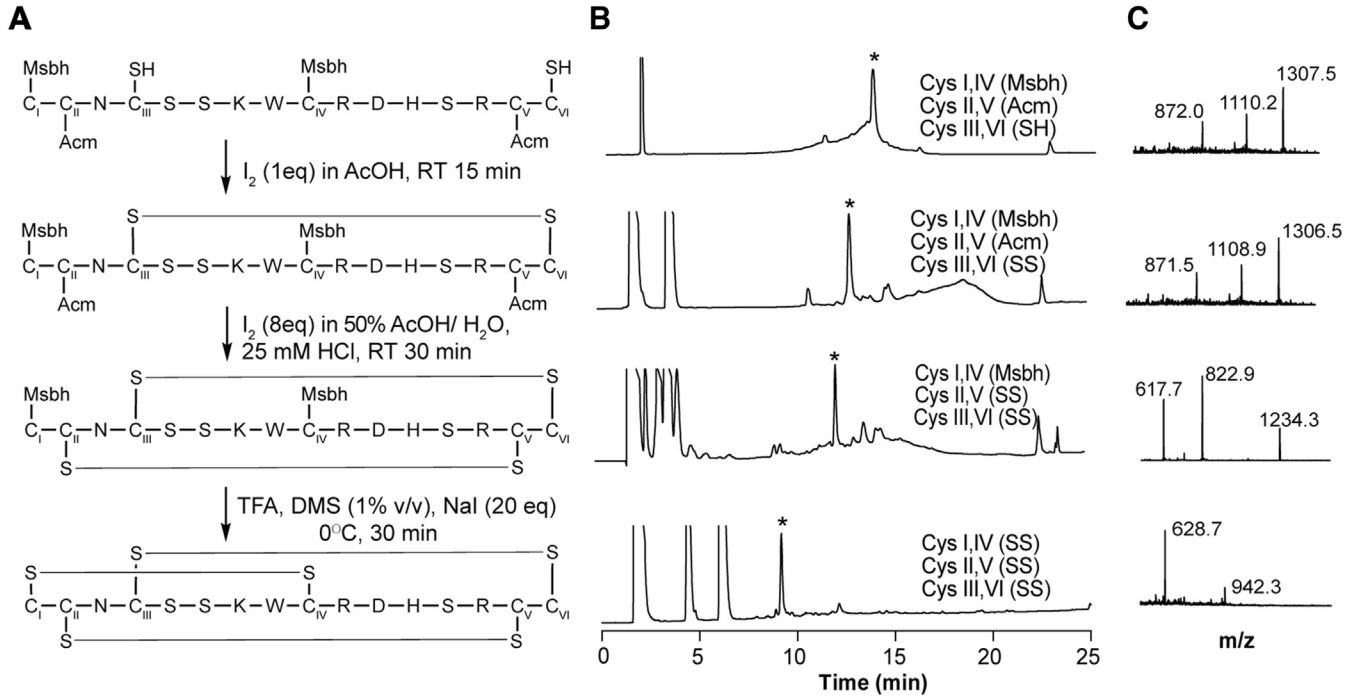

Figure 2. Regioselective synthesis of Native KIIIA (CysI-CysIV, CysII-CysV, CysIII-CysVI), forming disulfide bonds in the order of CysIII-CysVI, CysII-CysV, and CysI-CysIV. *A*, synthetic regioselective oxidation scheme showing reaction conditions for each step. *B*, analytical RP-HPLC traces corresponding to the product obtained by each step of the synthesis including the linear starting peptide, following the formation of first, second, and third disulfide bond. *C*, observed mass fragmentation corresponding to each folding step acquired by LC-MS. * denotes peptides of interest. RP-HPLC, reverse-phase HPLC.

Isomer 1-R (CysI-CysV, CysII-CysIV, CysIII-CysVI) KIIIA, confirming the results obtained by RP-HPLC and NMR (Figs. 1*B* and S5). In addition, the secondary Hα chemical shifts of Isomer 1-R superimposed well with chemical shifts from the structure of KIIIA published by Khoo *et al.* (Fig. S5*B*) (34), confirming that Isomer 1-T corresponds to the previously described structure with connectivity of CysI-CysV, CysII-CysIV, CysIII-CysVI.

In our hands, the minor peak obtained from thermodynamic folding, Isomer 2-T, coeluted with both Isomer 2-R (CysI-CysVI, CysII-CysIV, CysIII-CysV) and Native KIIIA (CysI-CysIV, CysII-CysV, CysIII-CysVI) produced regioselectively (Fig. 1*C*). However, using NMR, we could delineate the differences in their structures *via* 1D ^{1}H NMR spectra and secondary Hα chemical shifts (Fig. S5). 1D ^{1}H NMR spectra showed good dispersion of peaks in the order of Isomer 1 > Isomer 2 > Native. Isomer 1 was found to produce the highest quality spectrum with sharp peaks. Compared to Isomer 2, the Native isomer NMR spectra were not of similar sharpness and dispersion (Fig. S5*A*).

Activity and selectivity of KIIIA isomers at human Na_V channels

Evaluation of inhibitory activity and subtype selectivity of the three KIIIA isomers across $hNa_V1.2$, $hNa_V1.4$, and $hNa_V1.7$ by automated whole-cell patch-clamp electrophysiology (Fig. 3) provided insights into differences in activity displayed by the three different peptides. All three isomers inhibited $hNa_V1.2$, $hNa_V1.4$, and $hNa_V1.7$ with distinct potency and subtype selectivity (Fig. 3). Across hNa_V channels tested, Isomer 1 was the most potent inhibitor overall, followed by Native KIIIA and Isomer 2 (Table 2). However, the selectivity profiles of the three isomers showed preferential inhibition of $Na_V1.4$ over $Na_V1.2$ and $Na_V1.7$ by Isomer 1 ($Na_V1.4 > Na_V1.2 > Na_V1.7$), the Native isomer displayed selectivity for $Na_V1.4 > Na_V1.7 \approx Na_V1.2$, and Isomer 2 was approximately equipotent at $Na_V1.4$ and $Na_V1.2$ displaying diminished activity at $Na_V1.7$ ($Na_V1.4 \approx Na_V1.2 > Na_V1.7$).

Compared to Isomer 1, KIIIA Isomer 2 was more than 10-fold less active on $Na_V1.2$ ($p < 0.0002$), 31-fold less potent on $Na_V1.4$ ($p < 0.0002$), and 13-fold less active on $hNa_V1.7$ ($p < 0.0001$) (Table 2 and Fig. 3). On the other hand, Native KIIIA was more than 7-fold less active on $Na_V1.2$ and 10-fold less potent on $Na_V1.4$ while only being 2-fold less active on $hNa_V1.7$ compared to Isomer 1 (Table 2 and Fig. 3). These results demonstrate that disulfide connectivity can affect both potency and subtype selectivity and that the presumed native fold may not always be the most potent isoform at nonprey-specific pharmacological targets, or display the most desirable selectivity profile at human Na_V channels.

3D NMR structure of KIIIA isomers

To better understand factors driving the distinct potency and selectivity of the three KIIIA isomers, we investigated the 3D structures of Isomer 1, Isomer 2, and Native KIIIA (Fig. 4, *A–C*) using homonuclear ^{1}H NMR. TOCSY and NOESY spectra were used to assign individual spin systems and the sequential walk (45) in Ccpnmr (46). Intra-, inter-, and long-range NOEs were assigned for individual peptides, and an initial 20 structures were calculated using the AUTO function in Cyana followed by refinement in a watershell in CNS (47). Structural statistics for the three isomers were evaluated using Molmol (48) and MolProbity (49) and a family of 20 structures with the lowest energy and best MolProbity scores were chosen to represent each of the peptides (Table S3). The solution structures of Native KIIIA and KIIIA Isomer 2 have been submitted to the Protein Data Bank (KIIIA Native PDB ID: 7SAV and KIIIA Isomer 2 PDB ID: 7SAW) and the Bio-Magnetic Resonance Bank (KIIIA Native BMRB: 30953 and KIIIA Isomer 2 BMRB: 30954). All three isomers maintained the characteristic α-helix in the central loop of the peptide. Isomer 1 exhibited a very compact structure for μ-conotoxins, with a typical α-helical turn from Ser6 to Ser13 (34, 35). Native KIIIA also produced a very tight structure though its α-helix was observed to be shorter compared to Isomer 1, stretching from Ser6 to His12 (Fig. 4). Across the α-helical segment, the 3D structures of Isomer 1 and Native KIIIA were well structured with RMDS′ of 0.35 ± 0.1 Å and 0.4 ± 0.13 Å, respectively. The main difference between the two structures is noted in the N- and C-termini, which are oriented in different directions due to the constraint brought about by the cystine connectivity. Isomer 2 also displays an α-helical turn stretching from residue Ser6 to His12, though this helix (RMSD 0.54 ± 0.23 Å) exhibits more flexibility than Isomer 1 or Native, corresponding with fewer hydrogen bonds being observed across this stretch of amino acids for Isomer 2 (Table S3). Sidechain orientations residues which are responsible for interaction with the channels (36), such as Arg14, Ser13, His12, Asp11, Arg10 in Isomer 1 and Native KIIIA are similar, though these sidechains are orientated differently in Isomer 2 (Fig. 4, *A–C*). Overall, these structural differences, in particular, the shorter and more flexible helical structure of Isomer 2 (four hydrogen bonds in region Ser5–His12) compared to the compact α-helical structure of Isomer 1 and Native KIIIA (six hydrogen bonds each in the Ser6–His12 region), and the resultant changes in structural flexibility and sidechain positioning, could explain the relative decrease in potency observed for Isomer 2 in this study.

KIIIA isomers docking with $hNa_V1.2$

To begin to understand how these relatively minor structural differences might contribute to the observed functional differences, we further investigated the interactions of Isomer 1, Isomer 2, and Native KIIIA with $hNa_V1.2$ using the structure of $hNa_V1.2$ solved in combination with KIIIA, displaying a CysI-CysV, CysII-CysIV, CysIII-CysVI disulfide bond connectivity (Isomer 1-T), published by Pan *et al.* (PDB 6J8E) (50). The three isomers from this study were docked onto $hNa_V1.2$ containing a β2-subunit using Autodock VINA (51) and docking models with the lowest energy were chosen for further analysis. These docking studies confirmed that our Isomer 1-R and Native KIIIA (Fig. 4*D*), but not Isomer 2 (Fig. 4*E*), superimposed well with KIIIA in the $hNa_V1.2$ cryo-EM complex. Possible interactions between the residues of KIIIA

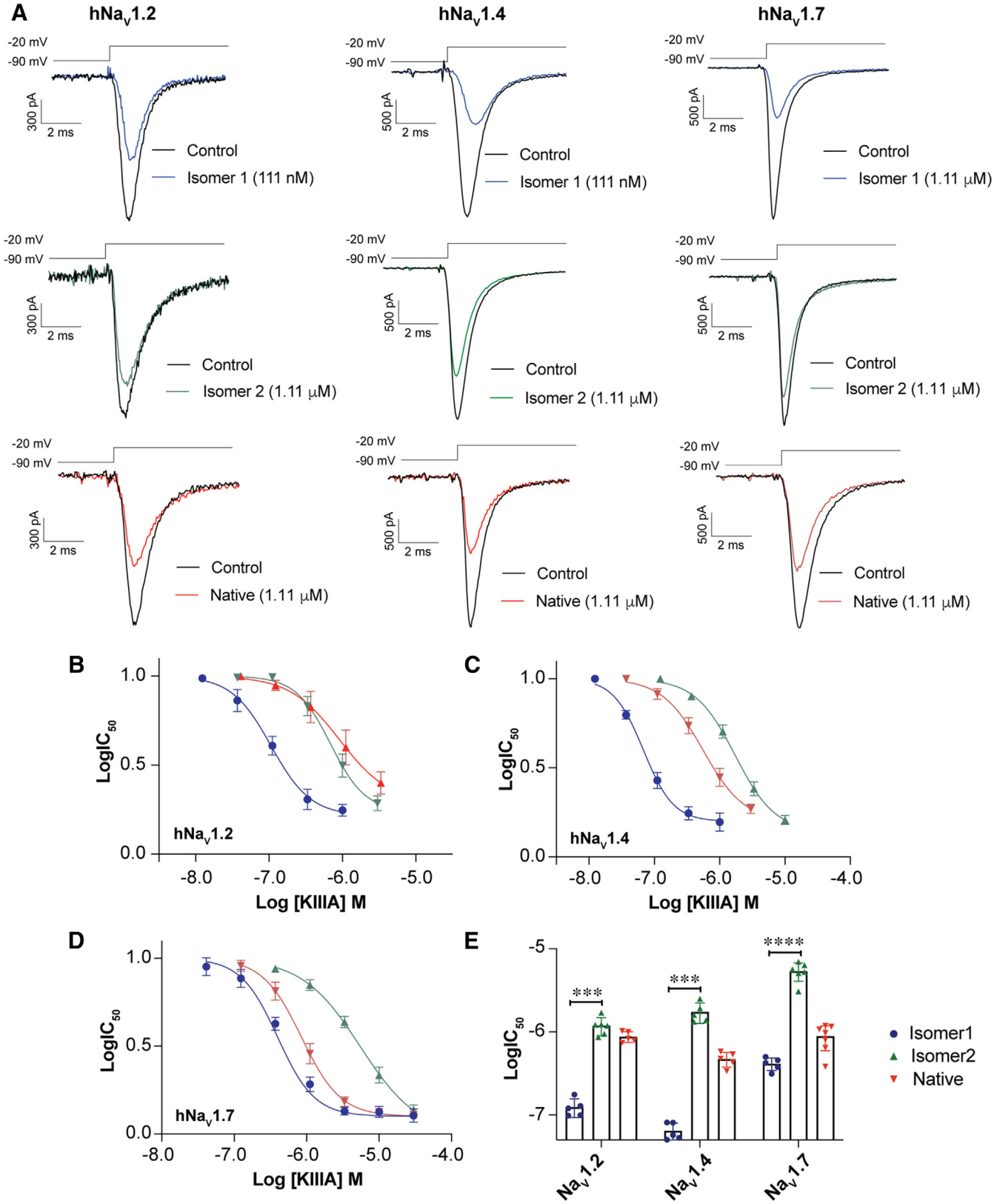

Figure 3. Pharmacology of KIIIA isomers at hNa$_V$ channels. *A*, representative current trace before and after the addition of Isomer 1 (*blue*), Isomer 2 (*green*), and Native KIIIA (*red*) at hNa$_V$1.2, hNa$_V$1.4, and hNa$_V$1.7. *B–D*, concentration-response curve showing inhibitory activity of KIIIA isomers at hNav1.2, hNa$_V$1.4, and hNa$_V$1.7 respectively, the data are presented as mean ± SEM. *E*, selectivity profile of KIIIA Isomer, Isomer 2, and Native acquired using automated whole-cell patch-clamp electrophysiology on HEK293 cells overexpressing hNa$_V$1.2, hNa$_V$1.4, or hNa$_V$1.7 in combination with β1-subunits. The data are presented as mean ± SD, with n = 5 cells per data point. 2-way ANOVA significance * p value < 0.0332, ** p value < 0.0021, *** p value < 0.0002, **** p value < 0.0001. NaV, voltage-gated sodium channel.

Table 2
Activity of KIIIA isomers on hNa$_V$1.2, hNa$_V$1.4, and hNa$_V$1.7 evaluated using automated electrophysiology

Sodium channel subtypes	Isomer 1	Isomer 2	Native KIIIA
hNa$_V$1.2	124 ± 34 nM	1371 ± 403 nM	875 ± 129 nM
hNa$_V$1.4	65 ± 15 nM	2051 ± 482 nM	472 ± 94 nM
hNa$_V$1.7	413 ± 71 nM	5388 ± 547 nM	887 ± 295 nM

The data are presented as mean ± SD, with n = 5 cells per data point.

isomers and hNa$_V$1.2 were identified by PDBsum (52) and are summarized in Figure 4*F* and Fig. S6. We first compared interactions in the Lys7–Ser13 region of docked Isomer 1 and the cryo-EM complex (50). There were multiple similarities between the two complexes, that is, Lys7 of KIIIA forms a hydrogen bond with Glu945 on hNa$_V$1.2, Trp8 interacts *via* nonbonded interactions with Tyr363, Arg10 interacts with Arg922 and Asp1426, Asp11 with Arg922, His12 with Ile914, Ser915, and Asp916, and Ser13 with Asn916, validating our docking study. Furthermore, when comparing the interactions of Isomer 1, Isomer 2, and the Native conformation of KIIIA with hNa$_V$1.2, we observed that Isomer 1 and the Native conformation KIIIA shared many interactions (Figs. 4*F* and S6). In contrast, Isomer 2 only shared two interactions with Isomer 1 and Native KIIIA, including His12 and Ser13 with Asn916. These differences and similarities between Native and Isomer 1/Isomer 2 could explain why Native KIIIA is more potent than Isomer 2 but less potent than Isomer 1 across the subtypes evaluated in this study. We also compared the interactions between residues in the termini of Isomer 1 and the Native KIIIA conformation with hNa$_V$1.2. Compared to the Native conformation of KIIIA, we noticed that Isomer 1 had two and three more interactions with the channel at the N- and C-terminus, respectively. These observations could explain why Isomer 1 is slightly more active at hNa$_V$1.2 than Native KIIIA. The results from these docking studies will need to be experimentally validated through structure-activity relationship studies of the peptide in combination with corresponding channel mutants and docking studies with Na$_V$1.4 and Na$_V$1.7 structures which may identify other important interactions.

Discussion

μ-Conotoxins, in particular KIIIA, have long been of interest as leads for novel analgesics due to their small size, chemical stability, and pharmacological profile (20, 29, 36). Like most μ-conotoxins, KIIIA displays activity at the neuronal Na$_V$1.2 and the skeletal muscle isoform Na$_V$1.4, which could be associated with adverse effects. However, KIIIA is one of only a few known μ-conotoxins exhibiting nanomolar potency at hNa$_V$1.7 (36, 50, 53–55). The KIIIA sequence was initially identified from a cDNA venom duct library from *C. kinoshitai* (31) and was subsequently chemically synthesized and folded thermodynamically, resulting in the formation of two disulfide bond isomers (Isomer 1; CysI-CysV, CysII-CysVI, CysIII-CysVI and Isomer 2; CysI-CysVI, CysII-CysIV, CysIII-CysV) as reported by Khoo *et al.* (35) However, it remains unclear which isomer(s) of KIIIA exist in *C. kinoshitai* venom (if it is present at all), what the 'real native' disulfide connectivity of the venom peptide is, and what machinery assists the snail with the folding of the peptide. Here, we report the regioselective synthesis of three KIIIA isomers, including for the first time KIIIA with the 'native' μ-conotoxins disulfide connectivity, their activity, selectivity, and their structure and interactions with human Na$_V$s.

Synthesis

While the development of an extensive repertoire of Cys-protecting groups has expanded the toolbox for regioselective oxidation of complex disulfide-rich peptides (56–63), complete orthogonal production of a peptide like KIIIA, containing three disulfide bonds (37.5% overall Cys content) is still not always straightforward. Directed synthesis of up to four disulfide bonds in a cysteine-rich peptide has been accomplished by using various protecting-group schemes with either Boc (*tert*-butoxycarbonyl) or Fmoc chemistry (63); most commonly with combinations of Trt, Acm, Mebzl, Mob, Msbh, *tert*butyl, or *S-tert*butylthio groups (56–63). Whereas the robustness of the Trt, Acm, and Mebzl or Mob protecting groups is established, the removal of *tert*butyl groups often results in the formation of side products and low yields (64–66), and the removal of *S-tert*butylthio groups by reducing agents has been observed to be sequence dependent (56, 67).

After trialing several different Cys-protecting groups following the preferential order of disulfide bond formation previously described (68–70) (Table S1), we successfully produced the three KIIIA isomers pursued in this study by regioselective chemical synthesis. By following a process described by Dekan *et al.* (63), using a combination of Trt/Acm/Msbh-protecting groups, we synthesized all three desired isomers with a yield of ∼10% calculated from the crude peptide. In general, regioselective oxidation methods are highly sequences dependent, meaning they may work for one peptide, but this may not always be transferable and work for other similar peptides.

Activity

μ-Conotoxins have previously been reported to mainly target Na$_V$1.4 and Na$_V$1.2 and only a few peptides, specifically KIIIA, SxIIIC, and CnIIIC, have been shown to target the therapeutically relevant isoform hNa$_V$1.7 (36, 50, 53–55, 71). In this study, we therefore focused our attention on these three sodium channel subtypes in order to investigate the activity and selectivity of Isomer 1, Isomer 2, and Native KIIIA. Previous selectivity and activity of KIIIA (Isomer 1) has been reported mainly for rat (20, 34, 72–74) and mouse Na$_V$ subtypes (29, 72), as well as some human Na$_V$ isoforms expressed in *Xenopus laevis* oocytes, with or without β subunits (50, 55, 72).

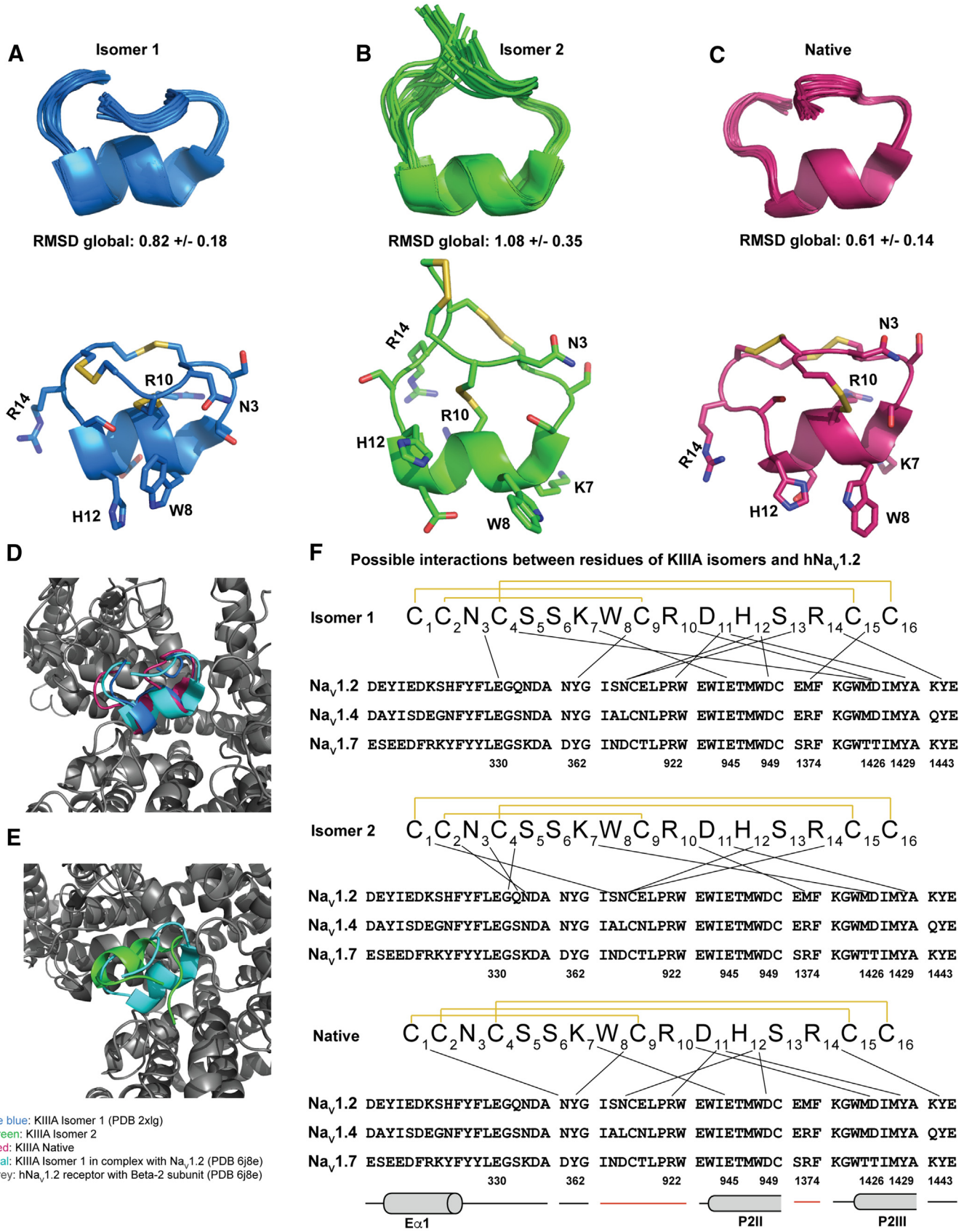

Figure 4. Three-dimensional structure of KIIIA isomers used in this study and docking studies with KIIIA-hNa$_V$1.2 complex (Pan *et al.* (PDB 6J8E) (50)**).** *A*, KIIIA Isomer 1 (PDB ID: 2XLG) (*blue*). *B*, KIIIA Isomer 2 (*green*) (this study). *C*, KIIIA Native (*red*) (this study). *D*, docked KIIIA Isomer 1 (*blue*) and Native KIIIA (*red*) compared to cryo-EM of KIIIA (Isomer 1, *teal*) in complex with hNa$_V$1.2. *E*, docked Isomer 2 (*green*) of KIIIA compared to cryo-EM of KIIIA (Isomer 1, *teal*) in complex with hNa$_V$1.2. *F*, putative interactions between KIIIA isomers and hNa$_V$1.2 compared to cryo-EM of KIIIA (Isomer 1) in complex with hNa$_V$1.2 (50). NaV, voltage-gated sodium channel.

The rank order of potency at human Na_V subtypes has not previously been reported, however Khoo *et al.* (29, 34, 35) and Wilson *et al.* (30) observed that Isomer 1 of KIIIA inhibits Na_Vs with a rank order of $rNa_V1.2 > rNa_V1.4 > mNa_V1.7 \geq rNa_V1.1 > rNa_V1.3 > rNa_V1.5$. Thus, the subtype selectivity preference for Isomer 1 of KIIIA across the human Na_V subtypes tested in this study is broadly consistent with the activity reported by these previous works. Although rat and human Na_V α-subunits are >95% identical at the level of amino acid sequence (75), species-specific activity differences have previously been reported for μ-conotoxins (29, 76, 77) and may account for some of the potency differences observed in this study compared to the literature.

Furthermore, coexpression of different β-subunits in heterologous expression systems can significantly affect affinity and efficacy of toxins, including μ-conotoxins (78, 79). Specifically, the on-rates (k_{on}) of μ-conotoxins at several Na_V channel isoforms can be increased in the presence of β1 and β3 subunits, while they are decreased by β2 and β4 subunits (80). In contrast, all four β-subunits increase the k_{on} of μO-conotoxin MrVIB (a gating-modifier inhibitor) at $Na_V1.8$ channels (29). Furthermore, coexpression of β2-or β4-subunits protects tetrodotoxin-sensitive $Na_V1.1$ to 1.7 subtypes against block by an analog of μO§-conotoxin GVIIJ (81). For KIIIA, coexpression of all rNa_V isoform except $Na_V1.5$ with β1 increased the rate of inactivation of I_{Na} (30).

Thus, to permit direct comparison of pharmacological activities of the three KIIIA isomers, we performed automated patch-clamp electrophysiology at human Na_V isoforms 1.2, 1.4, and 1.7 co-expressed in HEK cells with the β1-subunit. Consistent with the principal activity of many μ-conotoxins at $Na_V1.4$ and $Na_V1.2$, the KIIIA isomers were potent across these two isoforms. However, Native KIIIA displayed an improved relative selectivity for $Na_V1.7$ compared with Isomer 1 and Isomer 2 driven by a loss of activity at $Na_V1.4$ and $Na_V1.2$. As Na_V subtypes are characterized by a high degree of sequence identity ($hNa_V1.4$ cf. $hNa_V1.7$: 60.33% identical; $hNa_V1.2$ cf. $hNa_V1.7$: 77.11% identical; $hNa_V1.2$ cf. $hNa_V1.4$: 63.02% identical), similar functional characteristics, and a typical overall structure (5), these subtle shifts in potency and selectivity, driven by relatively modest shifts in the 3D peptide structure, remain difficult to explain. Recent advances in our understanding of the structure of Na_V channels, including a cryo-EM structure of KIIIA bound to human $Na_V1.2/β2$ (50) are particularly valuable in this regard and were thus used for docking studies to visualize putative interactions between key residues of different isomers of KIIIA with Na_V channels.

NMR and docking studies

Our experimentally determined Native KIIIA structure was highly similar across the α-helix part of the peptide compared to the structure of Isomer 1 (PDB ID: 2LXG) calculated by Khoo *et al.* (34, 35), consistent with the high degree of similarity between these two isomers. Due to the small size of KIIIA, the different disulfide connectivities of the three isomers had minimal effect on backbone of the structure, apart from across the N- and the C-terminus of KIIIA Isomer 2 structure (this study). However, the direction of the sidechains differed greatly, thus likely contributing to the different potency and selectivity profiles we observed.

Our docking studies also confirmed several critical interactions between KIIIA isomers and $Na_V1.2$ that were reported by previous studies (20, 36, 72, 82). Overall, the most pharmacologically similar isomers (Isomer 1 and Native KIIIA) had more interactions in common compared to Isomer 2, which was also considerably less potent across all Na_V subtypes studied. However, it is worth noting that these docking studies could be associated with some limitations. Firstly, both peptide NMR and the $Na_V1.2/β2$ cryo-EM structures may not reflect the full range of physiologically relevant conformations, which could contribute to subtle differences in activity. For example, our pharmacological activity studies were conducted in HEK293 cells coexpressing the β1-subunit, while the KIIIA-$hNa_V1.2$ cryo-EM structure was obtained in the presence of the β2-subunit (50). Additionally, the KIIIA-$Na_V1.2/β2$ cryo-EM structure was obtained with Biotin-(AEEA)2-KIIIA (Isomer 1) at very high peptide concentrations (25 mM) (50). Interestingly, although several interactions identified in the cryo-EM structure could explain preferential inhibition of $Na_V1.2$ over the tetrodotoxin-resistant isoforms $Na_V1.5$, $Na_V1.8$, and $Na_V1.9$, the even greater potency of KIIIA (Isomer 1) at $hNa_V1.4$, as well as potent activity at $hNa_V1.7$ observed by us, cannot be fully explained by this structure given that the majority of critical interacting residues are conserved across these subtypes.

We propose that the peptide N- and C-termini also contribute to differential interactions with Na_V subtypes, in addition to the helical region of KIIIA that has previously been identified to hold key residues accounting for μ-conotoxin activity at Na_V channels (20, 36, 72, 82). This is supported by previous work showing that both termini of KIIIA contribute to the interaction with $Na_V1.7$ and are sensitive to alterations (54). Specifically, the amidated C-terminus has proven critical for Isomer 1 KIIIA activity at $hNa_V1.7$, as both six amino acid C-terminal extension and deamidation resulted in complete loss of activity (54). In addition, an extension of the N-terminus of Isomer 1 KIIIA by a poly-Gly tail can either increase or decrease the potency of the peptide (35, 54). Contribution of the termini to the biological activity of KIIIA would also be consistent with the high degree of structural similarity of the isomers in the α-helical region, although this remains to be explored in greater detail at the practical level.

Conclusion

We produced three different disulfide bond isomers of KIIIA using a combination of thermodynamic and step-wise regioselective protocols evaluating a range of different Cys-protecting groups and disulfide bond formation order. We found that the combination and order of Cys(Trt), Cys(Acm), and Cys(Msbh) was the only strategy employed in this study, which was able to produce the desired folded peptides. Isomer 1, Isomer 2, and Native KIIIA were distinguishable *via* NMR, and although all three isomers share a similar overall 3D structure, comprising an α-helical turn locating from Lys7 to

His12, they displayed different potency and selectivity profiles across $hNa_V1.2$, $hNa_V1.4$, and $hNa_V1.7$. Docking of the 3D NMR structures revealed a series of interactions between the different KIIIA isomers and a $hNa_V1.2/\beta2$ complex that could provide an explanation for their distinct bioactivity. The docking study showed that while the α-helical turn and a series of hydrogen bonds are critical, both the N- and C-termini of KIIIA also appear to contribute to the interaction with hNa_V subtypes. Further experimental validation of such interactions may lead to the rational design of potent and selective $hNa_V1.7$ inhibitors with therapeutic potential.

Experimental procedures

Unless otherwise stated, all chemicals, solvents, and reagents were purchased from Sigma Aldrich (Sigma Aldrich). Amino acids were purchased from Iris Biotech GmbH.

Peptide synthesis

Peptides were manually assembled on Fmoc-Rink amide polystyrene resins on a 0.125 mmol scale (RAPP Polymer, 0.69 mmol/g). 9-fluorenylmethoxycarbonyl-protected amino acid couplings were performed in dimethylformamide using 4 eq of amino acid/0.5 M HCTU (O-(1H-6-Chlorobenzotriazole-1-yl)-1,1,3,3-tetramethyluronium hexafluorophosphate)/N,N-diisopropylamine (1:1:1) relative to resin substitution (2 × 10 min). 9-fluorenylmethoxycarbonyl removal was accomplished by treatment with 30% piperidine/dimethylformamide (2 × 2 min).

Cleavage from the resin and simultaneous removal of sidechain-protecting groups was accomplished by treatment with 95% TFA/2.5% triisopropylsilane/2.5% H_2O for 2 h at room temperature. Following the filtration of cleavage solution, ice-cold diethyl ether was added to precipitate peptides. Crude peptides were centrifuged 3 × 5 min at 5000*g*, washed with diethyl ether, dissolved in 0.1% TFA/50% acetonitrile (ACN)/H_2O, and lyophilized.

Reverse-phase HPLC

Preparative and analytical RP-HPLC Shimadzu LC-20AT systems equipped with an SPD-20A Prominence UV/VIS detector and a SIL-20AHT autoinjector were used for purification and analysis. An Eclipse XDB–C18 column (Agilent; 7 μm, 21.2 cm × 250 mm, 80 Å, flow rate 8 ml/min) was used for peptide purification. A Zobrax 300SB–C18 column (Agilent; 5 μm, 2.1 × 150 mm, 300 Å, flow rate 1 ml/min) was used to monitor oxidation and analyze the peptide purity. All samples were run from 0 to 60% B in 30 min (solvent A: 0.05% TFA and solvent B: 90% ACN/0.05% TFA). Absorbance was recorded at 214 nm and 280 nm.

Peptide oxidative folding

Linear KIIIA was thermodynamically folded as described previously (54). Briefly, linear unprotected KIIIA was dissolved in 0.1 M NH_4HCO_3, pH 8, at a concentration of 0.3 mg/ml with 100 eq GSH/10 eq GSSG and allowed to stir at room temperature for 24 h.

General procedures for removing cysteine-protecting groups and disulfide bond formation have been previously described by Dekan *et al.* (Figs. 1*A* and S1–S3). (63) Briefly, dithiol-containing peptide was dissolved in AcOH (2 mg/ml) following by the dropwise addition of 1 eq of aqueous iodine (I_2) in MeOH and kept stirring for 15 min to form the first disulfide bond. Subsequently, water and HCl were added to the above solution so that the final volume was 50% AcOH/50% H_2O/0.1% HCl. 8 eq of I_2 (dissolved in MeOH) was added to the peptide solution and stirred for 30 min to remove Acm group and form the second disulfide bond. The reactions were monitored by RP-HPLC and mass spectrometry. To stop the reaction, aqueous ascorbic acid was added to quench the I_2 until the solution became colorless. The product was isolated by RP-HPLC and lyophilized. The lyophilized bis(Cys(Msbh))-containing peptide was dissolved in TFA (1 mg/ml) and cooled to 0 °C (in an ice bath). Dimethyl sulfide (1% v/v) was added to the stirred solution, followed by NaI (5 eq/sulfoxide group). The solution gradually became yellow. After 15 min, the solution was poured into an ice-cold solution of 10 mM ascorbic acid in H_2O (15 × volume of TFA) and the product was isolated by RP-HPLC.

Liquid chromatography/mass spectrometry

A Q-Star Pulsar mass spectrometer (SCIEX) equipped with an auto-injector (Agilent Technologies Inc) was used for high-resolution mass analysis. A Zobrax 300SB – C18 column (Agilent; 3.5 μm, 2.1 × 100 mm, 300 Å, flow rate 0.3 ml/min) was used to run all samples. All runs were conducted in solvent A (0.1 % formic acid in H_2O) and solvent B (aqueous ACN/0.1 % formic acid).

Cell culture and automated patch-clamp electrophysiology

Automated whole-cell patch-clamp electrophysiology (QPatch-16X; Sophion A/S) was used to examine the activity of KIIIA isomers at $hNa_V1.2$, $hNa_V1.4$, and $hNa_V1.7$ as previously described (53). hNa_V subtypes 1.2, 1.4, and 1.7 (α and β1-subunits) were stably overexpressed in HEK293 cells (SB Drug Discovery). The cells were maintained in Minimum Essential Medium Eagle supplemented with 10% (*v/v*) fetal bovine serum, 1% (*v/v*) GlutaMAX, 0.004 mg/ml blasticidin, and 0.6 mg/ml geneticin.

The intracellular solution contained (in mM) 140 CsF, 1 EGTA, 5 CsOH, 10 Hepes, 10 NaCl, pH 7.3 and adjusted to 320 mOsm with sucrose. The extracellular solution comprised (in mM) 2 $CaCl_2$, 1 $MgCl_2$, 10 Hepes, 4 KCl, 145 NaCl, pH 7.4 and adjusted to 305 mOsm with sucrose. Voltage-clamp experiments were performed in a single-hole configuration mode. KIIIA isomers were diluted in extracellular solution with 0.1% bovine serum albumin. Na^+ currents were sampled at 25 kHz and filtered at 8 kHz. The same cells were exposed sequentially to multiples concentrations. Each peptide concentration was incubated for 5 min and the peak current was compared to buffer control. Concentration-response curves were acquired using a holding potential of −90 mV and a 50 ms pulse to −20 mV every 20 s (0.05 Hz). Peak current

postpeptide addition (I) was normalized to buffer control (I_0). IC_{50}s were determined by plotting difference in peak current (I/I_0) and log peptide concentration. Calculated IC_{50} were compared across subtypes and statistical differences determined by ordinary one-way ANOVA. Concentration-response curves were fitted using the log (inhibitor) *versus* response-variable slope (four parameters) and analyzed in Prism 8 (GraphPad Software).

NMR and 3D structure calculation

Peptides were dissolved in 500 µl MilliQ water (MilliPore) and 50 µl D_2O (Cambridge isotopes). A Bruker 600 MHz Avance III spectrometer equipped with a cryoprobe (Bruker) was used to acquire NMR spectra, as described by Agwa *et al.* (83) 1D ^1H, and 2D ^1H-^1H TOCSY (80 ms mixing time) and ^1H-^1H NOESY (200 ms mixing time), natural abundance ^1H–^{15}N HSQC and D_2O exchange 2D ^1H-^1H TOCSY and ^1H–^{13}C HSQC were collected (84, 85). Spectra were processed using TopSpin 3.5 (Bruker) and CCPNMR Analysis 2.4.1 (CCPN, University of Cambridge) (45, 46). The chemical shift of water at 4.76 ppm was used as a reference (86).

Dihedral angles were identified using TALOS-N (87), and initial 3D structures were calculated using the AUTO and ANNEAL functions in CYANA (88) followed by refinement in a watershell using CNS (47, 89). Additional H-bond restraints were included derived from temperature coefficient experiments in combination with D_2O exchange data (90). Fifty structures were calculated and the best 20 structures (based on energy and MolProbity scores (49)) were kept as the final 3D structure. Molmol (48) was used for visualization and RMSD calculations.

Docking and protein–protein interaction analysis

Autodock VINA software (51) assisted by MGLTools (91) was used for molecular docking of KIIIA isomers in human $Na_V1.2$ β2 cryo-EM structure (PDB 6J8E) (50). To define the search space of the $hNa_V1.2$ structure, a grid box with the following dimensions: center x = 143.432, center y = 136.254, and center z = 155.036 was used. The size of the grid box for all the docking in $hNa_V1.2$ was as follows: size x = 30, size y = 30, and size z = 30. The exhaustiveness for the search was set to 8. The lowest energy models were submitted and analyzed by PBDSum (52) for protein–protein interactions. PyMol was used for visualization.

Data availability

Supporting information includes orthogonal peptide oxidation, statistical analysis of NMR solution structures of Isomer 2 and Native KIIIA, regioselective oxidation, 1D and 2D ^1H NMR on Isomer 1, Isomer 2, and Native KIIIA, and putative-binding interactions between $Na_V1.2$ and Isomer 1, Isomer 2 and Native KIIIA can be found online. NMR coordinates for Isomer 2, and Native KIIIA solution structures have been submitted to the Protein Data Bank (KIIIA Isomer 2 PDB ID: 7SAW and KIIIA Native PDB ID: 7SAV) and the BioMagnetic Resonance Bank (KIIIA Isomer 2 BMRB: 30954 and KIIIA Native BMRB: 30953). All other data are included in the main article.

Supporting information—This article contains supporting information (34, 52, 63, 68–70, 86).

Acknowledgments—This work was funded by the Australian National Health and Medical Research Council (NMHRC) through Project and Ideas Grants (APP1080405, 2002860). The authors would like to thank Mr Zoltan Dekan from the Institute for Molecular Bioscience at the University of Queensland for invaluable advice and interesting peptide synthesis discussions and assistance with HF cleavage, Assoc Prof. Johan Rosengren from the School of Biomedical Sciences at the University of Queensland for assistance with NMR, and Ms Thao Ho from the Institute for Molecular Bioscience at the University of Queensland for advice with docking studies. This research was supported [in part] by the Intramural Research Program of the National Cancer Institute, Center for Cancer Research (Grant ZIA BC 012003).

Author contributions—H. N. T. T., I. V., and C. I. S. conceptualization; H. N. T. T. and C. I. S. methodology; H. N. T. T., K. L. M., J. R. D., and I. V. investigation; H. N. T. T. data curation; H. N. T. T. formal analysis; H. N. T. T. writing–original draft; H. N. T. T., I. V., and C. I. S. writing–review and editing; I. V. and C. I. S. supervision; I. V. and C. I. S. funding acquisition; I. V. and C. I. S. project administration.

Funding and additional information—This work was funded by a Career Development Fellowship (APP1162503) awarded to I. V. and an Early Career Fellowship (APP1139961) awarded to J. R. D. C. I. S was an Australian Research Council (ARC) Future Fellow (FT160100055). Australian Government Research Training Program Scholarships supported H. N. T. T. and K. L. M. through the University of Queensland.

Conflict of interest—The authors declare that they have no conflicts of interest with the contents of this article.

Abbreviations—The abbreviations used are: Acm, acetamidomethyl; ACN, acetonitrile; Fmoc, 9-fluorenylmethoxycarbonyl; Mebzl, 4-methylbenzyl; Mob, 4-methoxybenzyl; Msbh, 4,4′-dimethylsulfinylbenzhydryl; Na_V, voltage-gated sodium channel; PDB, Protein data bank; RP-HPLC, reverse-phase HPLC; Trt, S-triphenylmethyl.

References

1. Dib-Hajj, S. D., Black, J. A., and Waxman, S. G. (2009) Voltage-gated sodium channels: Therapeutic targets for pain. *Pain Med.* **10**, 1260–1269
2. Minett, M. S., Pereira, V., Sikandar, S., Matsuyama, A., Lolignier, S., Kanellopoulos, A. H., Mancini, F., Iannetti, G. D., Bogdanov, Y. D., Santana-Varela, S., Millet, Q., Baskozos, G., MacAllister, R., Cox, J. J., Zhao, J., *et al.* (2015) Endogenous opioids contribute to insensitivity to pain in humans and mice lacking sodium channel $Na_V1.7$. *Nat. Commun.* **6**, 1–16
3. Dib-Hajj, S. D., Black, J. A., and Waxman, S. G. (2015) $Na_V1.9$: A sodium channel linked to human pain. *Nat. Rev. Neurosci.* **16**, 511–519
4. Osteen, J. D., Herzig, V., Gilchrist, J., Emrick, J. J., Zhang, C., Wang, X., Castro, J., Garcia-Caraballo, S., Grundy, L., Rychkov, G. Y., Weyer, A. D., Dekan, Z., Undheim, E. A., Alewood, P., Stucky, C. L., *et al.* (2016) Selective spider toxins reveal a role for the $Na_V1.1$ channel in mechanical pain. *Nature* **534**, 494–499
5. Vetter, I., Deuis, J. R., Mueller, A., Israel, M. R., Starobova, H., Zhang, A., Rash, L. D., and Mobli, M. (2017) $Na_V1.7$ as a pain target - from gene to pharmacology. *Pharmacol. Ther.* **172**, 73–100

6. Bayburt, T. H., and Sligar, S. G. (2002) Single-molecule height measurements on microsomal cytochrome P450 in nanometer-scale phospholipid bilayer disks. *Epilepsy Res.* **99**, 6725–6730
7. Remme, C. A., and Bezzina, C. R. (2010) Sodium channel (dys)function and cardiac arrhythmias. *Cardiovasc. Ther.* **28**, 287–294
8. Catterall, W. A., Goldin, A. L., and Waxman, S. G. (2005) International Union of Pharmacology. XLVII. Nomenclature and structure-function relationships of voltage-gated sodium channels. *Pharmacol. Rev.* **57**, 397–409
9. Weiss, L. A., Escayg, A., Kearney, J. A., Trudeau, M., MacDonald, B. T., Mori, M., Reichert, J., Buxbaum, J. D., and Meisler, M. H. (2003) Sodium channels SCN1A, SCN2A and SCN3A in familial autism. *Mol. Psychiatry* **8**, 186–194
10. Planells-Cases, R., Caprini, M., Zhang, J., Rockenstein, E. M., Rivera, R. R., Murre, C., Masliah, E., and Montal, M. (2000) Neuronal death and perinatallethality in voltage-gated sodium channel alpha(II)-deficient mice. *Biophys. J.* **78**, 2878–2891
11. Boucher, T. J., Okuse, K., Bennett, D. L., Munson, J. B., Wood, J. N., and McMahon, S. B. (2000) Potent analgesic effects of GDNF inneuropathic pain states. *Science* **290**, 124–127
12. Hains, B. C., Klein, J. P., Saab, C. Y., Craner, M. J., Black, J. A., and Waxman, S. G. (2003) Upregulation of sodium channel $Na_V1.3$ and functional involvement in neuronal hyperexcitability associated with central neuropathic pain after spinal cord injury. *J. Neurosci.* **23**, 8881–8892
13. Burgess, D. L., Kohrman, D. C., Galt, J., Plummer, N. W., Jones, J. M., Spear, B., and Meisler, M. H. (1995) Mutation of a new sodium channel gene, Scn8a, in the mouse mutant "motor endplate disease.". *Nat. Genet.* **10**, 461–465
14. Lehmann-Horn, F., Jurkat-Rott, K., and Rudel, R. (2002) Periodic paralysis: Understanding channelopathie. *Curr. Neurol. Neurosci. Rep.* **2**, 61–69
15. Takahata, T., Yasui-Furukori, N., Sasaki, S., Igarashi, T., Okumura, K., Munakata, A., and Tateishi, T. (2003) Nucleotide changes in the translated region of SCN5A from Japanese patients with Brugada syndrome and control subjects. *Life Sci.* **72**, 2391–2399
16. Yang, Y., Wang, Y., Li, S., Xu, Z., Li, H., Ma, L., Fan, J., Bu, D., Liu, B., Fan, Z., Wu, G., Jin, J., Ding, B., Zhu, X., and Shen, Y. (2004) Mutations in SCN9A, encoding a sodium channel alpha subunit, in patients with primary erythermalgia. *J. Med. Genet.* **41**, 171–174
17. Akopian, A. N., Souslova, V., England, S., Okuse, K., Mcmahon, S. B., Boyce, S., Dickenson, A. H., and JN, W. (1999) The TTX-R sodium channel SNS has a specialized function in pain pathways. *Nat. Neurosci.* **2**, 541–548
18. Hoffmann, T., Sharon, O., Wittmann, J., Carr, R. W., Vyshnevska, A., Col, R., Nassar, M. A., Reeh, P. W., and Weidner, C. (2018) $Na_V1.7$ and pain: Contribution of peripheral nerves. *Pain* **159**, 496–506
19. Maxwell, M., Undheim, E. A. B., and Mobli, M. (2018) Secreted cysteine-rich repeat proteins "SCREPs": A novel multi-domain architecture. *Front. Pharmacol.* **9**, 1–16
20. Zhang, M. M., Han, T. S., Olivera, B. M., Bulaj, G., and Yoshikami, D. (2010) μ-Conotoxin KIIIA derivatives with divergent affinities *versus* efficacies in blocking voltage-gated sodium channels. *Biochemistry* **49**, 4804–4812
21. Payandeh, J., Scheuer, T., Zheng, N., and Catterall, W. A. (2011) The crystal structure of a voltage-gated sodium channel. *Nature* **475**, 353–358
22. Terlau, H., and Olivera, B. M. (2004) Conus venoms: A rich source of novel ion channel-targeted peptides. *Physiol. Rev.* **84**, 41–68
23. Kaas, Q., Westermann, J. C., Halai, R., Wang, C. K., and Craik, D. J. (2008) ConoServer, a database for conopeptide sequences and structures. *Bioinformatics* **24**, 445–456
24. Kaas, Q., Westermann, J. C., and Craik, D. J. (2010) Conopeptide characterization and classifications: An analysis using ConoServer. *Toxicon* **55**, 1491–1509
25. Corpuz, G. P., Jacobsen, R. B., Jimenez, E. C., Watkins, M., Walker, C., Colledge, C., Garrett, J. E., McDougal, O., Li, W., Gray, W. R., Hillyard, D. R., Rivier, J., McIntosh, J. M., Cruz, L. J., and Olivera, B. M. (2005) Definition of the M-conotoxin superfamily: Characterization of novel peptides from molluscivorous Conus venoms. *Biochemistry* **44**, 8176–8186
26. Shon, K.-J., Olivera, B. M., Watkins, M., Jacobsen, R. B., Gray, W. R., Floresca, C. Z., Cruz, L. J., Hillyard, D. R., Brink, A., Terlau, H., and Yoshikami, D. (1998) μ-Conotoxin PIIIA, a new peptide for discriminating among tetrodotoxin-sensitive Na channel subtypes. *J. Neurosci.* **18**, 4473–4481
27. Tietze, A. A., Tietze, D., Ohlenschlager, O., Leipold, E., Ullrich, F., Kuhl, T., Mischo, A., Buntkowsky, G., Gorlach, M., Heinemann, S. H., and Imhof, D. (2012) Structurally diverse μ-conotoxin PIIIA isomers block sodium channel Na_V 1.4. *Angew. Chem. Int. Ed. Engl.* **51**, 4058–4061
28. Dutton, J. L., Bansal, P. S., Hogg, R. C., Adams, D. J., Alewood, P. F., and Craik, D. J. (2002) A new level of conotoxin diversity, a non-native disulfide bond connectivity in α-conotoxin AuIB reduces structural definition but increases biological activity. *J. Biol. Chem.* **277**, 48849–48857
29. Wilson, M. J., Yoshikami, D., Azam, L., Gajewiak, J., Olivera, B. M., Bulaj, G., and Zhang, M. M. (2011) μ-Conotoxins that differentially block sodium channels $Na_V1.1$ through 1.8 identify those responsible for action potentials in sciatic nerve. *Proc. Natl. Acad. Sci. U. S. A.* **108**, 10302–10307
30. Knapp, O., McArthur, J. R., and Adams, D. J. (2012) Conotoxins targeting neuronal voltage-gated sodium channel subtypes: Potential analgesics? *Toxins* **4**, 1236–1260
31. Bulaj, G., West, P. J., Garrett, J. E., Watkins, M., Zhang, M. M., Norton, R. S., Smith, B. J., Yoshikami, D., and Olivera, B. M. (2005) Novel conotoxins from Conus striatus and Conus *kinoshitai* selectively block TTX-resistant sodium channels. *Biochemistry* **44**, 7259–7265
32. Stevens, M., Peigneur, S., and Tytgat, J. (2011) Neurotoxins and their binding areas on voltage-gated sodium channels. *Front. Pharmacol.* **2**, 71
33. King, G. F., Escoubas, P., and Nicholson, G. M. (2008) Peptide toxins that selectively target insect Na_V and C_V channels. *Channels* **2**, 100–116
34. Khoo, K. K., Feng, Z. P., Smith, B. J., Zhang, M. M., Yoshikami, D., Olivera, B. M., Bulaj, G., and Norton, R. S. (2009) Structure of the analgesic μ-conotoxin KIIIA and effects on the structure and function of disulfide deletion. *Biochemistry* **48**, 1210–1219
35. Khoo, K. K., Gupta, K., Green, B. R., Zhang, M. M., Watkins, M., Olivera, B. M., Balaram, P., Yoshikami, D., Bulaj, G., and Norton, R. S. (2012) Distinct disulfide isomers of μ-conotoxins KIIIA and KIIIB block voltage-gated sodium channels. *Biochemistry* **51**, 9826–9835
36. McArthur, J. R., Singh, G., McMaster, D., Winkfein, R., Tieleman, D. P., and French, R. J. (2011) Interactions of key charged residues contributing to selective block of neuronal sodium channels by μ-conotoxin KIIIA. *Mol. Pharmacol.* **80**, 573–584
37. Barton, M. E., and White, H. S. (2004) The effect of CGX-1007 and CI-1041, novel NMDA receptor antagonists, on kindling acquisition and expression. *Epilepsy Res.* **59**, 1–12
38. Cruz, L. J., Kupryszewski, G., LeCheminant, G. W., Gray, W. R., Olivera, B. M., and Rivier, J. (1989) μ-Conotoxin GIIIA, a peptide ligand for muscle sodium channels: Chemical synthesis, radiolabeling, and receptor characterization. *Biochemistry* **28**, 3437–3442
39. Green, B. R., Bulaj, G., and Norton, R. S. (2014) Structure and function of μ-conotoxins, peptide-based sodium channel blockers with analgesic activity. *Future Med. Chem.* **6**, 1677–1698
40. Kim, K., and Seong, B. L. (2001) Peptide amidation: Production of peptide hormones *in vivo* and *in vitro*. *Biotechnol. Bioprocess Eng.* **6**, 244–251
41. McIntosh, J. M., Hasson, A., Spira, M. E., Gray, W. R., Li, W., Marsh, M., Hillyard, D. R., and Olivera, B. M. (1995) A new family of conotoxins that blocks voltage-gated sodium channels. *J. Biol. Chem.* **270**, 16796–16802
42. Miljanich, G. P. (2004) Ziconotide: Neuronal calcium channel blocker for treating severe chronic pain. *Curr. Med. Chem.* **11**, 3029–3040
43. Sharpe, I. A., Palant, E., Schroeder, C. I., Kaye, D. M., Adams, D. J., Alewood, P. F., and Lewis, R. J. (2003) Inhibition of the norepinephrine transporter by the venom peptide χ-MrIA. Site of action, Na+ dependence, and structure-activity relationship. *J. Biol. Chem.* **278**, 40317–40323
44. Staats, P. S., Yearwood, T., Charapata, S. G., Presley, R. W., Wallace, M. S., Byas-Smith, M., Fisher, R., Bryce, D. A., Mangieri, E. A., Luther, R. R., Mayo, M., McGuire, D., and Ellis, D. (2004) Intrathecal ziconotide in the

treatment of refractory pain in patients with cancer or AIDS: A randomized controlled trial. *JAMA* **291**, 63–70
45. Wüthrich, K. (1986) *NMR of Proteins and Nucleic Acids*, Wiley Interscience, New York, NY
46. Vranken, W. F., Boucher, W., Stevens, T. J., Fogh, R. H., Pajon, A., Llinas, M., Ulrich, E. L., Markley, J. L., Ionides, J., and Laue, E. D. (2005) The CCPN data model for NMR spectroscopy: Development of a software pipeline. *Proteins* **59**, 687–696
47. Brunger, A. T., Adams, P. D., Clore, G. M., DeLano, W. L., Gros, P., Grosse-Kunstleve, R. W., Jiang, J. S., Kuszewski, J., Nilges, M., Pannu, N. S., Read, R. J., Rice, L. M., Simonson, T., and Warren, G. L. (1998) Crystallography & NMR system: A new software suite for macromolecular structure determination. *Acta Crystallogr. D Biol. Crystallogr.* **54**, 905–921
48. Koradi, R., Billeter, M., and Wuthrich, K. (1996) MOLMOL: A program for display and analysis of macromolecular structures. *J. Mol. Graph.* **14**, 29–32
49. Chen, V. B., Arendall, W. B., 3rd, Headd, J. J., Keedy, D. A., Immormino, R. M., Kapral, G. J., Murray, L. W., Richardson, J. S., and Richardson, D. C. (2010) MolProbity: All-atom structure validation for macromolecular crystallography. *Acta Crystallogr. D Biol. Crystallogr.* **66**, 12–21
50. Pan, X., Li, Z., Huang, X., Huang, G., Gao, S., Shen, H., Liu, L., Lei, J., and Yan, N. (2019) Molecular basis for pore blockade of human Na(+) channel $Na_V1.2$ by the μ-conotoxin KIIIA. *Science* **363**, 1309–1313
51. Trott, O., and Olson, A. J. (2010) AutoDock vina: Improving the speed and accuracy of docking with a new scoring function, efficient optimization, and multithreading. *J. Comput. Chem.* **31**, 455–461
52. Laskowski, R. A., Jablonska, J., Pravda, L., Varekova, R. S., and Thornton, J. M. (2018) PDBsum: Structural summaries of PDB entries. *Protein Sci.* **27**, 129–134
53. McMahon, K. L., Tran, H. N. T., Deuis, J. R., Lewis, R. J., Vetter, I., and Schroeder, C. I. (2020) Discovery, pharmacological characterisation and NMR structure of the novel μ-conotoxin SxIIIC, a potent and irreversible Na_V channel inhibitor. *Biomedicines* **8**, 391–406
54. Tran, H. N. T., Tran, P., Deuis, J. R., Agwa, A. J., Zhang, A. H., Vetter, I., and Schroeder, C. I. (2020) Enzymatic ligation of a pore blocker toxin and a gating modifier toxin: Creating double-knotted peptides with improved sodium channel $Na_V1.7$ inhibition. *Bioconjug. Chem.* **31**, 64–73
55. Knuhtsen, A., Whiting, R., McWhinnie, F. S., Whitmore, C., Smith, B. O., Green, A. C., Timperley, C. M., Kinnear, K. I., and Jamieson, A. G. (2020) μ-Conotoxin KIIIA peptidomimetics that block human voltage-gated sodium channels. *Pept. Sci.* **113**, 1–11
56. Eliasen, R., Andresen, T. L., and Conde-Frieboes, K. W. (2012) Handling a tricycle: Orthogonal *versus* random oxidation of the tricyclic inhibitor cystine knotted peptide gurmarin. *Peptides* **37**, 144–149
57. Wu, F., Mayer, J. P., Gelfanov, V. M., Liu, F., and DiMarchi, R. D. (2017) Synthesis of four-disulfide insulin analogs *via* sequential disulfide bond formation. *J. Org. Chem.* **82**, 3506–3512
58. Gali, H., Sieckman, G. L., Hoffman, T. J., Owen, N. K., Mazuru, D. G., Forte, L. R., and Volkert, W. A. (2002) Chemical synthesis of Escherichia coli ST(h) analogues by regioselective disulfide bond formation: Biological evaluation of an (111)In-DOTA-Phe(19)-ST(h) analogue for specific targeting of human colon cancers. *Bioconjug. Chem.* **13**, 224–231
59. Boulegue, C., Musiol, H.-J., Prasad, V., and Moroder, L. (2007) Synthesis of cystine-rich Pp. *ChemInform* **38**, 24–36
60. Vetter, I., Dekan, Z., Knapp, O., Adams, D. J., Alewood, P. F., and Lewis, R. J. (2012) Isolation, characterization and total regioselective synthesis of the novel μO-conotoxin MfVIA from Conus magnificus that targets voltage-gated sodium channels. *Biochem. Pharmacol.* **84**, 540–548
61. Jin, A. H., Dekan, Z., Smout, M. J., Wilson, D., Dutertre, S., Vetter, I., Lewis, R. J., Loukas, A., Daly, N. L., and Alewood, P. F. (2017) Conotoxin Φ-MiXXVIIA from the superfamily G2 employs a novel cysteine framework that mimics granulin and displays anti-apoptotic activity. *Angew. Chem. Int. Ed. Engl.* **56**, 14973–14976
62. Deuis, J. R., Dekan, Z., Inserra, M. C., Lee, T. H., Aguilar, M. I., Craik, D. J., Lewis, R. J., Alewood, P. F., Mobli, M., Schroeder, C. I., Henriques, S. T., and Vetter, I. (2016) Development of a μO-conotoxin analogue with improved lipid membrane interactions and potency for the analgesic sodium channel $Na_V1.8$. *J. Biol. Chem.* **291**, 11829–11842
63. Dekan, Z., Mobli, M., Pennington, M. W., Fung, E., Nemeth, E., and Alewood, P. F. (2014) Total synthesis of human hepcidin through regioselective disulfide-bond formation by using the safety-catch cysteine protecting group 4,4'-dimethylsulfinylbenzhydryl. *Angew. Chem. Int. Ed. Engl.* **53**, 2931–2944
64. Kluver, E., Schulz-Maronde, S., Scheid, S., Meyer, B., Forssmann, W. G., and Adermann, K. (2005) Structure-activity relation of human β-defensin 3: Influence of disulfide bonds and cysteine substitution on antimicrobial activity and cytotoxicity. *Biochemistry* **44**, 9804–9816
65. Schulz, A., Kluver, E., Schulz-Maronde, S., and Adermann, K. (2005) Engineering disulfide bonds of the novel human β-defensins hBD-27 and hBD-28: Differences in disulfide formation and biological activity among human β-defensins. *Biopolymers* **80**, 34–49
66. Szabo, I., Schlosser, G., Hudecz, F., and Mezo, G. (2007) Disulfide bond rearrangement during regioselective oxidation in $PhS(O)Ph/CH_3SiCl_3$ mixture for the synthesis of α-conotoxin GI. *Biopolymers* **88**, 20–28
67. Denis, B., and Trifilieff, E. (2000) Synthesis of palmitoyl-thioester T-cell epitopes of myelin proteolipid protein (PLP). Comparison of two thiol protecting groups (StBu and Mmt) for on-resin acylation. *J. Pept. Sci.* **6**, 372–377
68. Norton, R. S., and Pallaghy, P. K. (1998) The cystine knot structure of ion channel toxins and related polypeptides. *Toxicon* **36**, 1573–1583
69. Pallaghy, P. K., Nielsen, K. J., Craik, D. J., and Norton, R. S. (1994) A common structural motif incorporating a cystine knot and a triple-stranded beta-sheet in toxic and inhibitory polypeptides. *Protein Sci.* **3**, 1833–1839
70. Agwa, A. J., Tran, P., Mueller, A., Tran, H. N. T., Deuis, J. R., Israel, M. R., McMahon, K. L., Craik, D. J., Vetter, I., and Schroeder, C. I. (2020) Manipulation of a spider peptide toxin alters its affinity for lipid bilayers and potency and selectivity for voltage-gated sodium channel subtype 1.7. *J. Biol. Chem.* **295**, 5067–5080
71. Markgraf, R., Leipold, E., Schirmeyer, J., Paolini-Bertrand, M., Hartley, O., and Heinemann, S. H. (2012) Mechanism and molecular basis for the sodium channel subtype specificity of μ-conopeptide CnIIIC. *Br. J. Pharmacol.* **167**, 576–586
72. Van Der Haegen, A., Peigneur, S., and Tytgat, J. (2011) Importance of position 8 in μ-conotoxin KIIIA for voltage-gated sodium channel selectivity. *FEBS J.* **278**, 3408–3418
73. Catterall, W. A. (2000) From ionic currents to molecular mechanisms: The structure and function of voltage-gated sodium channels. *Neuron* **26**, 13–25
74. He, B., and Soderlund, D. M. (2014) Functional expression of rat $Na_V1.6$ voltage-gated sodium channels in HEK293 cells: Modulation by the auxiliary β1 subunit. *PLoS One* **9**, e85188
75. Goldin, A. L., Barchi, R. L., Caldwell, J. H., Hofmann, F., Howe, J. R., Hunter, J. C., Kallen, R. G., Mandel, G., Meisler, M. H., Netter, Y. B., Noda, M., Tamkun, M. M., Waxman, S. G., Wood, J. N., and Catterall, W. A. (2000) Nomenclature of voltage-gated sodium channels. *Neuron* **28**, 365–368
76. West, P. J., Bulaj, G., Garrett, J. E., Olivera, B. M., and Yoshikami, D. (2002) μ-conotoxin SmIIIA, a potent inhibitor of tetrodotoxin-resistant sodium channels in amphibian sympathetic and sensory neurons. *Biochemistry* **41**, 15388–15393
77. Keizer, D. W., West, P. J., Lee, E. F., Yoshikami, D., Olivera, B. M., Bulaj, G., and Norton, R. S. (2003) Structural basis for tetrodotoxin-resistant sodium channel binding by μ-conotoxin SmIIIA. *J. Biol. Chem.* **278**, 46805–46813
78. Gilchrist, J., Das, S., Van Petegem, F., and Bosmans, F. (2013) Crystallographic insights into sodium-channel modulation by the β4 subunit. *Proc. Natl. Acad. Sci. U. S. A.* **110**, 5016–5024
79. Namadurai, S., Yereddi, N. R., Cusdin, F. S., Huang, C. L., Chirgadze, D. Y., and Jackson, A. P. (2015) A new look at sodium channel β subunits. *Biol. Open* **5**, 1–12
80. Zhang, M. M., Wilson, M. J., Azam, L., Gajewiak, J., Rivier, J. E., Bulaj, G., Olivera, B. M., and Yoshikami, D. (2013) Co-expression of Na_V β subunits

alters the kinetics of inhibition of voltage-gated sodium channels by pore-blocking μ-conotoxins. *Br. J. Pharmacol.* **168**, 1597–1610
81. Gajewiak, J., Azam, L., Imperial, J., Walewska, A., Green, B. R., Bandyopadhyay, P. K., Raghuraman, S., Ueberheide, B., Bern, M., Zhou, H. M., Minassian, N. A., Hagan, R. H., Flinspach, M., Liu, Y., Bulaj, G., *et al.* (2014) A disulfide tether stabilizes the block of sodium channels by the conotoxin μO section sign-GVIIJ. *Proc. Natl. Acad. Sci. U. S. A.* **111**, 2758–2763
82. Zhang, M. M., Green, B. R., Catlin, P., Fiedler, B., Azam, L., Chadwick, A., Terlau, H., McArthur, J. R., French, R. J., Gulyas, J., Rivier, J. E., Smith, B. J., Norton, R. S., Olivera, B. M., Yoshikami, D., *et al.* (2007) Structure/function characterization of μ-conotoxin KIIIA, an analgesic, nearly irreversible blocker of mammalian neuronal sodium channels. *J. Biol. Chem.* **282**, 30699–30706
83. Agwa, A. J., Blomster, L. V., Craik, D. J., King, G. F., and Schroeder, C. I. (2018) Efficient enzymatic ligation of inhibitor cystine knot spider venom peptides: Using sortase a to form double-knottins that probe voltage-gated sodium channel $Na_V1.7$. *Bioconjug. Chem.* **29**, 3309–3319
84. Braunschweiler, L., and Ernst, R. R. (1983) Coherence transfer by isotropic mixing - application to proton correlation spectroscopy. *J. Magn. Reson.* **53**, 521–528
85. Jeener, J., Meier, B. H., Bachmann, P., and Ernst, R. R. (1979) Investigation of exchange processes by two-dimensional NMR spectroscopy. *J. Chem. Phys.* **71**, 4546–4553
86. Gottlieb, H. E., Kotlyar, V., and Nudelman, A. (1997) NMR chemical shifts of common laboratory solvents as trace impurities. *J. Org. Chem.* **62**, 7512–7515
87. Shen, Y., and Bax, A. (2013) Protein backbone and sidechain torsion angles predicted from NMR chemical shifts using artificial neural networks. *J. Biomol. NMR* **56**, 227–241
88. Gottstein, D., Kirchner, D. K., and Guntert, P. (2012) Simultaneous single-structure and bundle representation of protein NMR structures in torsion angle space. *J. Biomol. NMR* **52**, 351–364
89. Brunger, A. T. (2007) Version 1.2 of the crystallography and NMR system. *Nat. Prot.* **2**, 2728–2733
90. Baxter, N. J., and Williamson, M. P. (1997) Temperature dependence of ^1H chemical shifts in proteins. *J. Biomol. NMR* **9**, 359–369
91. Morris, G. M., Huey, R., Lindstrom, W., Sanner, M. F., Belew, R. K., Goodsell, D. S., and Olson, A. J. (2009) AutoDock4 and AutoDockTools4: Automated docking with selective receptor flexibility. *J. Comput. Chem.* **30**, 2785–2791
92. Wang, C. Z., Zhang, H., Jiang, H., Lu, W., Zhao, Z. Q., and Chi, C. W. (2006) A novel conotoxin from Conus striatus, μ-SIIIA, selectively blocking rat tetrodotoxin-resistant sodium channels. *Toxicon* **47**, 122–132
93. Schroeder, C. I., Ekberg, J., Nielsen, K. J., Adams, D., Loughnan, M. L., Thomas, L., Adams, D. J., Alewood, P. F., and Lewis, R. J. (2008) Neuronally μ-conotoxins from Conus striatus utilize an α-helical motif to target mammalian sodium channels. *J. Biol. Chem.* **283**, 21621–21628
94. Cruz, L. J., Gray, W. R., Olivera, B. M., Zeikus, R. D., Kerr, L., Yoshikami, D., and Moczydlowski, E. (1985) Conus geographus toxins that discriminate between neuronal and muscle sodium channels. *J. Biol. Chem.* **260**, 9280–9288
95. Holford, M., Zhang, M. M., Gowd, K. H., Azam, L., Green, B. R., Watkins, M., Ownby, J. P., Yoshikami, D., Bulaj, G., and Olivera, B. M. (2009) Pruning nature: Biodiversity-derived discovery of novel sodium channel blocking conotoxins from Conus bullatus. *Toxicon* **53**, 90–98
96. Zhang, M. M., Fiedler, B., Green, B. R., Catlin, P., Watkins, M., Garrett, J. E., Smith, B. J., Yoshikami, D., Olivera, B. M., and Bulaj, G. (2006) Structural and functional diversities among μ-conotoxins targeting TTX-resistant sodium channels. *Biochemistry* **45**, 3723–3732